International Journal of Modern Manufacturing Technologies
ISSN 2067–3604, Vol. XII, No. 1 / 2020

# INVESTIGATIONS OF LASER MACHINING PARAMETERS USING RSM AND OPTIMIZATION TECHNIQUES FOR HASTELLOY C-276

**Sagar Hiwale, Rajiv Basavarajappa**

College of Engineering Pune, Department of Production Engineering and Industrial Management, Pune- 411005, India

Corresponding author: Sagar Hiwale, hiwalesagar@gmail.com

***Abstract:*** Laser cutting is a leading cutting-edge thermal based industrial process used as a substitute to traditional mechanical cutting processes. In this paper, an experimental investigation is carried out using CNC controlled Prima 4000W CW-$CO_2$ laser cutting on Hastelloy C- 276 using Response surface methodology (RSM). The laser process parameters such as laser power, cutting speed, gas pressure, working distance and focal position are considered to obtain the influence on selected performance characteristics kerf width and kerf taper. The second order regression models are developed for considered performance characteristics using the experimental results. The ANOVA analysis is performed to obtain the significant laser process parameter for kerf width and kerf taper. Two swarm based optimization techniques, i.e., black hole (BH) and krill herd (KH) algorithm are used to obtain the optimum parameter setting for the considered laser machining process. The effectiveness of the KH algorithm is found better compared to BH algorithm for the considered process. The result obtained using RSM and optimization techniques are confirmed using confirmatory tests with percentage of error less than 5 %. The confirmatory test shows that the considered approaches are effective in optimizing the parameters of laser machining process.

***Key words :*** $CO_2$ based laser machining, Hastelloy C-276, response surface method, kerf taper, black hole algorithm, krill herd algorithm

## 1. INTRODUCTION

Laser machining technology is a non-contact thermal based process incorporated in the manufacturing industry for its selected applications in cutting of difficult to hard materials. Laser machining process has different process parameters that have a considerable influence on the laser cut quality like, kerf width and kerf taper. The selection of these laser process parameters is important as it has utmost significant to obtain the desired quality of kerf characteristics. With the advancement in the field of metallurgy, metal alloys are being extensively used in the engineering sector, well-known examples being the Nickel-based alloys [1, 2]. Among Ni-based alloys, Hastelloy C-276 as a nickel-molybdenum-chromium super alloy with well corrosion- resistance which is comprehensively applied in the chemical and nuclear industries recently [3]. The applications of super alloy are wide-ranging such as chemical processing, pollution control, pulp and paper production, industrial and municipal waste treatment, etc. In this work, Hastelloy C-276 is machined using laser machining technology to obtain the optimum process parameter setting for desired quality of cut.

In the literature, Manikandana et al. [4] has reported the microstructure study of weldments produced on material C-276 using gas tungsten arc welding process. Pusavec et al. [5] have reported the sustainable machining of material Nickel based alloy – Inconel 718 using cryogenics based machining process to enhance the cutting condition like, power consumption and cutting forces. Another study of Altin et al. [6] has reported the experimental investigation on material Inconel 718 to demonstrate the effects of parameter cutting speed on tool wear and life. A review study on the machinability of nickel-based alloys and other materials using different machining methods with its applications is reported [7-9]. In selected study, the assessment of economical way for machining hard alloys using non-contact machining tools is reported [10,11]. Ghany and Newishy [12] has performed experimental investigation to optimize the laser process parameters which enhance the response suface roughness (Ra) and kerf characteristics during machining of austenitic stainless steel using CW Nd:YAG laser beam. A brief study on the exploration of the capability and applications of the Laser beam machining is reported to provide future direction of research in terms of opportunities and obstacles lies with machinability of difficult to hard materials [13, 14]. Wang et al. [15] have carried out experimental investigation with selected settings of laser process parameters using laser heat assisted machining to analyse responses like, cutting force, tool wear and Ra during machining of material aluminum matrix composite ($Al_2O_3p/Al$).

Hascalık and Ay [16] has performed the experimental investigation using RSM to obtain the effects of laser parameters on selected responses like, surface roughness (Ra) kerf taper ratio, recast layer thickness for material Inconel 718 Nickel based alloy. It is observed that laser power has more influence on output characteristics compared to cutting speed. Eltawahni et al. [17] has investigated the effects of $CO_2$ laser cutting parameters of laser power, gas pressure, cutting speed, nozzle diameter and focus point position on the kerf characteristics for material stainless steel with grade AISI316L. An optimal cutting setting was obtained using the RSM approach. Yilbas [18] has studied the $CO_2$ laser cutting of mild steel using the statistical method based on the factorial analysis to identify the influence of laser cutting parameters on the desired kerf quality.

An experimental investigation was performed experiments on Inconel-718 using pulsed Nd:YAG laser beam and the objective function, i.e., geometrical quality was optimized using swarm based optimization technique “particle swarm optimization” [19]. Shrivastava and Pandey [20] have reported the multi-objective optimization of the kerf deviation, kerf width and kerf taper in the laser cutting of Inconel-718 using Nd:YAG laser incorporated with compressed gas to achieve special quality of cut. An investigation is carried out to inspect the quality of laser cutting with respect to process parameters like, laser power, scanning speed, pulsing frequency and the gas pressure using $CO_2$ laser cut for the aluminum alloy AA5083 material [21].

Kotadiya et al. [22] have attempted parametric analysis on laser machining process parameters like laser power, cutting speed and gas pressure during machining of stainless steel (ASTM 304) and they have observed that laser power has substantial effect on Ra and top kerf. Joshi and Sharma [23] have performed experimental investigation on pulsed Nd-YAG laser using Box Behnken design to analyse kerf geometry and metallurgical variation in material aluminum alloy (Al 6061-T6) with selected settings of lamp current, pulse width, pulse frequency and cutting speed. Boujelbene [24] has found cutting speed and laser power as the significant parameter using analysis of variance for Ra during machining of carbon steel sheet (S235). An experimental investigation is performed using $CO_2$ laser cutting during profile cutting of gears made of material stainless steel 304 to obtain the influence of parameters such as power, cutting speed, focal position and gas pressure on performance characteristic Ra [25].

An investigation using ANOVA analysis was performed to obtain the percentage contribution of cutting parameters of $CO_2$ laser such as laser power, cutting speed and gas pressure on output characteristics Ra and kerf width for material SS-304 [26]. Sharifi and Akbari [27] has carried out experimental investigation on CO2 laser cutting of material Al 6061 T6 alloy to determine the effects of laser process parameters like speed, laser power, standoff distance and sheet thickness on temperature and cutting edge quality. It is found that laser power has substantial effect on considered output characteristics. Elsheikh et al. [28] have attempted experimental investigation using RSM to obtain the influence of cutting parameters like, cutting speed, gas pressure, laser beam power and sheet thickness on the cutting quality for the material Poly methyl methacrylate sheets. The genetic algorithm is attempted to obtain the optimum parameter setting of the considered laser process parameter to enhance the cutting quality.

In this paper, an experimental investigation is attempted to determine optimum condition for laser machining process parameters. The work focused on the laser machining of material Hastelloy C276, whose applications are found in chemical process equipment’s, evaporator, exchanger, sour gas vessel, pump-fan housing, food processing equipment’s, system of flue gas desulfurization. Subsequently, RSM with ANOVA analysis is applied to obtain the influence of laser machining process parameters (laser power, cutting speed, gas pressure, working distance and focal position) on kerf width and kerf taper angle using rotable central composite design of experiment. Furthermore, to obtain the approximate optimum condition of Laser machining process parameters selected soft computing evolutionary optimization techniques, such as black hole (BH), and krill herd (KH) algorithm are applied to the second order regression models. The applicability of the considered algorithms makes possible to study the effects of associated laser machining process parameter with respect to the considered performance characteristics, i.e., kerf width and kerf taper.

## 2. EXPERIMENT SETUP AND MATERIAL

The experiment were conducted on the prima 4000W CW $CO_2$ laser cutting system connected with CNC work table as depicted in Figure 1. The experimental setup was used to analyze the effects of significant parameters laser power, cutting speed, gas pressure, working distance and focal position during machining using Laser cutting on required performance characteristics kerf width and kerf taper. The geometrical features like, kerf width and kerf taper are shown in Figure 2. The workpiece material “Hastelloy C276” was used for the experimentation having 3.7 mm thickness. The chemical composition of the selected material “Hastelloy C276” is 16.5 % Mo, 6.2 % Fe, 3.11 % W, 0.11 % V, 0.6 % Mn, 0.087 % Co, 0.034 % Si, 0.001 % S, 0.004 % P, 15.5 % Cr and balance Ni. A conical shaped nozzle which is co-axial to the laser beam was used to blow the gas mixture on to the workpiece material. The experiment conductions were in the form of a continuous cutting regime conditions with nitrogen gas used as an assist gas. All the experiment runs are carried out using same nozzle with 2.5 mm diameter with nitrogen gas at constant flow rate. For the experiment purpose, the focal length of selected lens was kept at 190.5 mm.

Fig. 1. Laser beam cutting machine setup

The selection of the control factors (process parameters of considered laser machining process) in the experiment is important aspect as they have significant influence on the output characteristics. In the present investigation, the control factors selected are the laser power, cutting speed, gas pressure, working distance and focal position. The range of the considered five control factors with their corresponding levels are shown in Table 1. With the help of the pilot experimentation, the ranges and levels of control factors are determined. The output characteristics kerf width and kerf taper are selected to see the influence of selected control parameters.

Table 1. Range and Levels of the process parameters

| Process parameter | Unit | Level | | | | |
|---|---|---|---|---|---|---|
| | | -1 | -0.42 | 0 | +0.42 | +1 |
| Laser power | watt | 2400 | 2805.69 | 3100 | 3394.31 | 3800 |
| Cutting Speed | mm/min | 1125 | 1494.46 | 1762.50 | 2030.54 | 2400 |
| Gas Pressure | bar | 11 | 12.74 | 14 | 15.26 | 17 |
| Working Distance | mm | 0.5 | 0.79 | 1 | 1.21 | 1.50 |
| Focus Position | mm | -4.2 | -2.84 | -1.85 | -0.86 | 0.5 |

Specimens are prepared using sandpaper with 60–600 mesh was used to grind the close surface texture of machined surface. At the end of grinding process, the surfaces were cleaned and polished using diamond paste and solvent. The aquaregia solution consists of 5 ml nitric acid ($HNO_3$) and 15ml hydro chloric acid (HCl) was used to etch the polished specimens. The layout of the experiment plan designed using rotable central composite second order with experimental results obtained are shown in Table 2.

Table 2. Experiment results

| Laser power (watt) | Cutting speed (mm/min) | Gas pressure (bar) | Working Distance (mm) | Focus Position (mm) | Kerf width (mm) | Kerf taper (degree) |
|---|---|---|---|---|---|---|
| 3394.31 | 1494.46 | 12.74 | 0.79 | -2.84 | 0.463 | 0.189 |
| 3394.31 | 1494.46 | 15.26 | 1.21 | -0.86 | 0.495 | -0.122 |
| 3394.31 | 2030.54 | 12.74 | 1.21 | -2.84 | 0.439 | 0.325 |
| 3100.00 | 1762.50 | 14.00 | 1.00 | 0.50 | 0.532 | 0.173 |
| 3394.31 | 1494.46 | 15.26 | 0.79 | -0.86 | 0.498 | -0.183 |
| 3100.00 | 1762.50 | 14.00 | 1.00 | -4.20 | 0.455 | 0.407 |
| 2805.69 | 1494.46 | 12.74 | 1.21 | -2.84 | 0.436 | 0.175 |
| 3394.31 | 1494.46 | 15.26 | 1.21 | -2.84 | 0.448 | 0.261 |
| 3100.00 | 1762.50 | 14.00 | 1.00 | -1.85 | 0.453 | 0.173 |
| 3100.00 | 1762.50 | 14.00 | 1.50 | -1.85 | 0.478 | -0.138 |
| 3100.00 | 1762.50 | 14.00 | 1.00 | -1.85 | 0.474 | 0.134 |
| 3100.00 | 1762.50 | 17.00 | 1.00 | -1.85 | 0.478 | -0.032 |
| 2805.69 | 1494.46 | 12.74 | 1.21 | -0.86 | 0.488 | 0.101 |
| 2805.69 | 2030.54 | 15.26 | 1.21 | -0.86 | 0.470 | 0.027 |
| 2805.69 | 1494.46 | 15.26 | 1.21 | -2.84 | 0.455 | 0.238 |
| 3100.00 | 1762.50 | 14.00 | 1.00 | -1.85 | 0.470 | 0.214 |
| 2805.69 | 2030.54 | 12.74 | 0.79 | -0.86 | 0.472 | 0.312 |
| 3394.31 | 1494.46 | 12.74 | 1.21 | -0.86 | 0.493 | 0.232 |
| 2805.69 | 1494.46 | 15.26 | 1.21 | -0.86 | 0.482 | 0.020 |
| 2805.69 | 2030.54 | 15.26 | 0.79 | -0.86 | 0.454 | 0.185 |
| 3100.00 | 1762.50 | 14.00 | 1.00 | -1.85 | 0.484 | 0.173 |
| 3394.31 | 2030.54 | 15.26 | 1.21 | -2.84 | 0.455 | 0.387 |
| 3100.00 | 1125.00 | 14.00 | 1.00 | -1.85 | 0.465 | 0.203 |
| 2805.69 | 1494.46 | 12.74 | 0.79 | -0.86 | 0.489 | 0.331 |
| 3100.00 | 1762.50 | 14.00 | 0.50 | -1.85 | 0.457 | 0.076 |
| 3394.31 | 1494.46 | 12.74 | 1.21 | -2.84 | 0.468 | 0.345 |
| 2805.69 | 2030.54 | 12.74 | 1.21 | -0.86 | 0.473 | 0.132 |
| 3394.31 | 1494.46 | 15.26 | 0.79 | -2.84 | 0.475 | 0.087 |
| 3100.00 | 2400.00 | 14.00 | 1.00 | -1.85 | 0.435 | 0.266 |
| 2400.00 | 1762.50 | 14.00 | 1.00 | -1.85 | 0.425 | 0.382 |
| 3100.00 | 1762.50 | 14.00 | 1.00 | -1.85 | 0.467 | 0.163 |
| 3394.31 | 2030.54 | 12.74 | 0.79 | -0.86 | 0.492 | 0.339 |
| 3100.00 | 1762.50 | 14.00 | 1.00 | -1.85 | 0.467 | 0.067 |
| 2805.69 | 1494.46 | 15.26 | 0.79 | -0.86 | 0.500 | 0.005 |
| 3100.00 | 1762.50 | 14.00 | 1.00 | -1.85 | 0.464 | 0.304 |
| 3100.00 | 1762.50 | 14.00 | 1.00 | -1.85 | 0.454 | 0.133 |
| 3100.00 | 1762.50 | 14.00 | 1.00 | -1.85 | 0.459 | 0.296 |
| 3394.31 | 1494.46 | 12.74 | 0.79 | -0.86 | 0.503 | 0.122 |
| 3394.31 | 2030.54 | 12.74 | 0.79 | -2.84 | 0.450 | 0.409 |
| 3394.31 | 2030.54 | 12.74 | 1.21 | -0.86 | 0.491 | 0.405 |
| 2805.69 | 2030.54 | 12.74 | 1.21 | -2.84 | 0.435 | 0.231 |
| 3394.31 | 2030.54 | 15.26 | 0.79 | -0.86 | 0.505 | -0.142 |
| 3394.31 | 2030.54 | 15.26 | 0.79 | -2.84 | 0.447 | 0.223 |
| 3800.00 | 1762.50 | 14.00 | 1.00 | -1.85 | 0.466 | 0.392 |
| 2805.69 | 1494.46 | 15.26 | 0.79 | -2.84 | 0.435 | 0.390 |
| 2805.69 | 2030.54 | 15.26 | 0.79 | -2.84 | 0.426 | 0.557 |
| 3100.00 | 1762.50 | 11.00 | 1.00 | -1.85 | 0.462 | 0.294 |
| 2805.69 | 2030.54 | 15.26 | 1.21 | -2.84 | 0.435 | 0.411 |
| 2805.69 | 1494.46 | 12.74 | 0.79 | -2.84 | 0.431 | 0.252 |
| 3394.31 | 2030.54 | 15.26 | 1.21 | -0.86 | 0.477 | 0.033 |
| 3100.00 | 1762.50 | 14.00 | 1.00 | -1.85 | 0.447 | 0.311 |
| 2805.69 | 2030.54 | 12.74 | 0.79 | -2.84 | 0.433 | 0.443 |

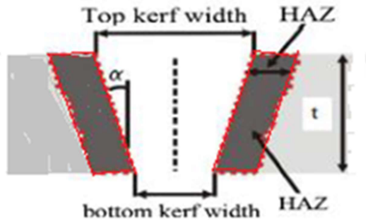

Fig. 2. Geometrical features the *kerf* characteristics

During the experimentation, a 15 mm long straight cut is made on each specimen to determine the desired output characteristics. The specimen samples produced using the experimentation is shown in Figure 2. To measure the average of bottom kerf width from the specimen, five different locations were selected along the length of cut on the specimen bottom face. An equipment stereo zoom microscope was utilized to measure kerf width. It has trinocular body with objective lens zoom range of 0.65 X- 4.5 X and working distance up to 100 mm.

## 3. METHODOLOGY

Response surface method (RSM) is used to build the regression models for the experimental results. The experiments are the series of runs for the independent variables, i.e., laser power, cutting speed, working distance and focus position which are used to obtain the influence on the responses like kerf width and kerf tape. The RSM method reduces the experimental runs compared to other methods like full factorial without degrading the actual objective and thus reduces the cost of experiments. The main objective is to obtain the optimal values that are governed by the independent variables. The general second order equation for obtaining the values of models is given in equation (1)

$$y = \beta_0 + \sum_{l=1}^{k} \beta_i x_i + \sum_{l=1}^{k} \beta_{ii} x_{ii}^2 + \sum_i \sum_j \beta_{ij} x_i x_j + \varepsilon \qquad (1)$$

Where, y is the response, $x_i$ is the $i^{th}$ machining parameter, $b$ is the regression coefficients, ε is the error during the experiment.

The second term in equation (1) signifies the linear effect (main factor effects), second sigma notation represents the quadratic effects whereas the third term signifies the higher order two-factor interaction effects. By using a least square technique, the values of the coefficient can be obtained (Montogomery, 2010; Paneerselvam, 2012). In order to obtain the influence of each factor and interactions, the RSM is a suitable choice owing to its capability. In order to analyze the response characteristics like, kerf width and kerf taper, second order regression models are developed. A rotable central composite second order quadratic design with 52 experimental runs is used to conduct the experimentation. Using the experimental results as given in Table 2, the final second order regression models in coded form obtained for the considered characteristics, i.e., kerf width and kerf taper are given in equations (2) - (3).

$$\boldsymbol{kerf\ width} = 0.46404 + 0.02107\,x_1 - 0.0153\,x_2 + 0.00229\,x_3 + 0.00088\,x_4 + 0.04597\,x_5 - 0.01780\,x_1^2 - 0.01345\,x_2^2 + 0.00660\,x_3^2 + 0.0037\,x_4^2 + 0.03025\,x_5^2 + 0.0057\,x_1x_2 + 0.0002\,x_1x_3 - 0.0054\,x_1x_5 - 0.0058\,x_2x_3 + 0.0046\,x_2x_4 - 0.004\,x_2x_5 - 0.0023\,x_3x_4 - 0.0070\,x_3x_5 - 0.0102\,x_4x_5 \qquad (2)$$

$$\boldsymbol{kerf\ taper} = 0.2570 + 0.120\,x_1 + 0.053\,x_2 + 0.004\,x_3 + 0.016\,x_4 + 0.001\,x_5 + 0.133\,x_1^2 + 0.098\,x_2^2 + 0.032\,x_3^2 + 0.045\,x_4^2 + 0.008\,x_5^2 - 0.322\,x_1x_2 + 0.037\,x_1x_3 - 0.021x_1x_5 + 0.036\,x_2x_3 + 0.068\,x_2x_4 + 0.016\,x_2x_5 + 0.050\,x_3x_4 + 0.094\,x_3x_5 + 0.044\,x_4x_5 \qquad (3)$$

Where, $x_1$ is laser power (watts), $x_2$ is cutting speed (mm/min), $x_3$ is gas pressure (bar), $x_4$ is working distance (mm) and $x_5$ is focal position (mm).
In the next section, the analysis of variance (ANOVA) analysis is used to check the adequacy of the developed regression models for kerf width and kerf taper. The ANOVA is carried out to obtain the influence of the selected laser machining process parameters on the considered responses. The detailed result and discussion for the effects of process parameters are given as under.

### 3.1 Analysis of kerf width

The ANOVA results for the obtained quadratic model of kerf width are shown in Table 3. It is found from Table 3 that the model is significant as the obtained F-value is 41.90. The Table 3 reveals that the model terms along with square terms of laser power ($x_1$), cutting speed ($x_2$), working distance ($x_4$), focus position ($x_5$) and interaction terms i.e., $x_1x_4$ , $x_2x_3$, $x_3$ $x_5$ are significant as the value of "Prob > F" is less than 0.05. The corresponding F-value of each term i.e., linear, squared and interaction are reported in Table 3, the term with higher F-value would have the more significance. From Table 3, it is observed that the F-value of focus position is 428.7 which are higher compared to other parameters. It reveals from Table 3 that the parameter focus position has higher effects on kerf width followed by parameter laser power. With reference to F-value, the parameter gas pressure and working distance with F-value as 2.6 and 5 respectively has least effect on kerf width. The obtained value of "Pred R-Squared" as 0.8952 shows good agreement with the value of "Adj R-Squared" as 0.9413 i.e. the difference found to be less than 0.2.

As the value of laser power increases the performance characteristic kerf width is increased (Figure 3 (a-b)). The machining time is reduced with the increase of laser power and thus the worker may select high laser power. The higher value of laser power may deter the quality of kerf width. It is revealed from the Figure 3(a) that the maximum kerf width is achieved at 3800 watts laser power, 1762.5 mm/min cutting speed, 14 bar gas pressure, 1 mm working distance and - 4.2 mm focus position.

Table 3. ANOVA analysis of *kerf width*

| ***Source*** | ***Sum of Squares*** | ***Degree of freedom*** | ***Mean Square*** | ***F Value*** | ***p-value Prob > F*** |
|---|---|---|---|---|---|
| Model | 20 | 0.0234 | 0.001174 | 41.9 | <0.001 |
| Linear | 5 | 0.0175 | 0.003503 | 125.0 | <0.001 |
| Laser power $(x_1)$ | 1 | 0.0034 | 0.003406 | 121.5 | <0.001 |
| Cutting speed $(x_2)$ | 1 | 0.0018 | 0.001877 | 67.0 | <0.001 |
| Gas pressure $(x_3)$ | 1 | 0.0001 | 0.000073 | 2.6 | 0.117 |
| Working distance $(x_4)$ | 1 | 0.0002 | 0.000141 | 5.0 | 0.032 |
| Focus position $(x_5)$ | 1 | 0.0120 | 0.012016 | 428.7 | <0.001 |
| **2-Way Interaction** | 10 | 0.0001 | 0.000091 | 3.3 | 0.006 |
| $x_1 x_2$ | 1 | 0 | 0 | 0.0 | 0.947 |
| $x_1x_3$ | 1 | 0.000004 | 0.000004 | 0.2 | 0.692 |
| $x_1x_4$ | 1 | 0.000220 | 0.000220 | 7.9 | 0.009 |
| $x_1x_5$ | 1 | 0.000072 | 0.000072 | 2.6 | 0.119 |
| $x_2x_3$ | 1 | 0.000149 | 0.000149 | 5.3 | 0.028 |
| $x_2 x_4$ | 1 | 0.000032 | 0.000032 | 1.1 | 0.294 |
| $x_2 x_5$ | 1 | 0.000025 | 0.000025 | 0.9 | 0.357 |
| $x_3x_4$ | 1 | 0.000067 | 0.000067 | 2.4 | 0.133 |
| $x_3 x_5$ | 1 | 0.000307 | 0.000307 | 11.0 | 0.002 |
| $x_4x_5$ | 1 | 0.000036 | 0.000036 | 1.3 | 0.265 |
| Error | 31 | 0.000869 | 0.000028 | | |
| Lack-of-Fit | 22 | 0.000594 | 0.000027 | 0.9 | 0.617 |
| Pure Error | 9 | 0.000275 | 0.000031 | | |
| Total | 51 | 0.024343 | | | |
| S: 0.0052943 | $R^2$: 96.43% | | $R^2$(adjacent): 94.13% $R^2$(predicted): 89.52% | | |

The effects of laser power on kerf width with respect to focus position and cutting speed are shown in Figures 3(a) and (b). It is observed from Figure 3(a) as the focus position (locating the laser spot point in the depth of the specimen) decreases the performance characteristics kerf width decreases. The removal of material occurs due to concentration of laser at the cutting zone. As the focus position increases the concentration of laser energy is increased that reduce the indentation of the laser energy during machining results improved kerf width.

It is observed from the Figure 3(b) as the cutting speed increases; there is a gradual decrease (little effect is observed) in the performance characteristics *kerf width*. This is due to the fact that, as the cutting speed increases the interaction of laser energy with workpiece material would get less time for producing the machining cut result in decrease of *kerf top width*. It is concluded that the maximum *kerf width* occurs at the maximum laser power and minimum cutting speed. It is observed from the Table 3 that the gas pressure and working distance with F-value as 2.6 and 5 has little effect on kerf width during the machining of material Hastelloy C-276 using laser machining process. Furthermore, the *p* – value as reported in Table 3 in the ANOVA analysis reveals their insignificance for the response *kerf width*.

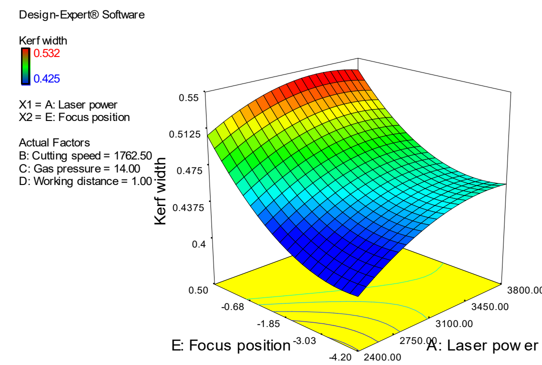


(a)

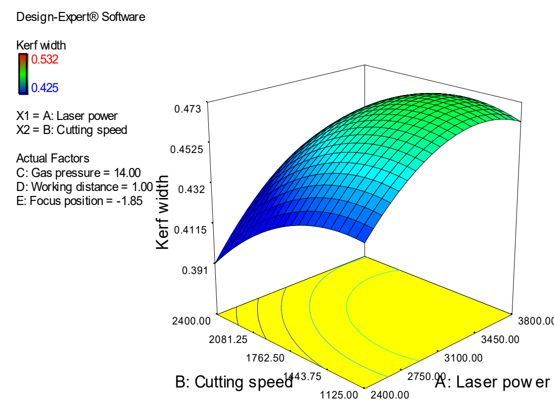


(b)

**Fig. 3.** Response surface plots of *kerf width* for significant process parameters **(a)** focus position and laser power, **(b)** cutting speed and laser power.

## 3.2 Analysis of kerf taper

The ANOVA results for the obtained quadratic model of kerf taper are shown in Table 4. It is found from Table 4 that the model is found to be significant as the obtained F-value is 143.5. From Table 4, it reveals that the model terms along with square terms of laser power($x_1$), cutting speed ($x_2$), working distance ($x_4$) and interaction terms i.e., $x_1x_2$, $x_1x_3$, $x_2x_3$, $x_2x_4$, $x_3x_4$, $x_3x_5$, $x_1x_2$, $x_1x_4$, $x_4x_5$ are significant as the value of "Prob > F" is less than 0.05. The corresponding F-value of each term i.e., linear, squared and interaction are reported in Table 4, the term with higher F-value would have the more significance. From Table 4, it is observed that the F-value of laser power is 938.8 which are higher compared to other parameters. It reveals from Table 4 that the parameter laser power has higher effects on kerf taper followed by parameter cutting speed. With reference to F-value, the parameter gas pressure, working distance and focus position with

F-value as 1.1, 17.5 and 0.1 respectively has least effect on kerf taper. The obtained value of "Pred R-Squared" as 0.9743 shows good agreement with the value of "Adjacent R-Squared" as 0.9824 i.e., the difference found to be less than 0.2.

Table 4. ANOVA analysis of *kerf taper*

| *Source* | *Sum of Squares* | *Degree of freedom* | *Mean Square* | *F Value* | *p-value Prob > F* |
|---|---|---|---|---|---|
| Model | 20 | 0.3110 | 0.01555 | 143.5 | <0.001 |
| Linear | 5 | 0.1236 | 0.02472 | 228.1 | <0.001 |
| Laser power *($x_1$)* | 1 | 0.1017 | 0.10175 | 938.8 | <0.001 |
| Cutting speed *($x_2$)* | 1 | 0.0198 | 0.01984 | 183.1 | <0.001 |
| Gas pressure *($x_3$)* | 1 | 0.0001 | 0.00012 | 1.1 | 0.297 |
| Working distance *($x_4$)* | 1 | 0.00189 | 0.00189 | 17.5 | 0.070 |
| Focus position *($x_5$)* | 1 | 0.00001 | 0.00001 | 0.1 | 0.752 |
| **2-Way** | 10 | 0.13174 | 0.01317 | 121.6 | <0.001 |
| $x_1 x_2$ | 1 | 0.10399 | 0.10399 | 959.4 | <0.001 |
| $x_1x_3$ | 1 | 0.00202 | 0.00202 | 18.7 | <0.001 |
| $x_1x_4$ | 1 | 0.00011 | 0.00011 | 1.1 | 0.309 |
| $x_1x_5$ | 1 | 0.00045 | 0.00045 | 4.2 | 0.050 |
| $x_2x_3$ | 1 | 0.00188 | 0.00188 | 17.4 | <0.001 |
| $x_2 x_4$ | 1 | 0.00461 | 0.00461 | 42.6 | <0.001 |
| $x_2 x_5$ | 1 | 0.00024 | 0.00024 | 2.2 | 0.144 |
| $x_3x_4$ | 1 | 0.00363 | 0.00363 | 33.5 | <0.001 |
| $x_3 x_5$ | 1 | 0.01285 | 0.01285 | 118.6 | <0.001 |
| $x_4x_5$ | 1 | 0.00194 | 0.00194 | 17.9 | <0.001 |
| Error | 31 | 0.00336 | 0.00010 | | |
| Lack-of-Fit | 22 | 0.00168 | 0.00007 | 0.4 | 0.957 |
| Pure Error | 9 | 0.00167 | 0.00018 | | |
| Total | 51 | 0.31438 | | $R^2$(predicted): 97.43% | |
| S: 0.0104 | $R^2$: | $R^2$(adjacent): | | | |

When Continuous Wave $CO_2$ laser straight cutting process is used and to maintain quality and accuracy of cut, low value of kerf taper is desirable. Therefore, during laser machining of considered material Hastelloy C276, the influence of significant laser machining process parameters on kerf taper is shown in Figure 4 (a-c). It is observed that kerf taper occurs during the cutting operation is due to the uneven laser beam profile which is an inherent characteristics of a laser machining process. The presence of kerf taper is found in major cases of laser cut specimens, but it can be reduced by proper selection of laser process parameters. Kerf width measurements at the top and bottom surfaces indicates that the top kerf width is slightly larger than bottom kerf for most of the cutting conditions due to loss of beam intensity, loss of gas pressure and defocusing of beam across the thickness of the workpiece material.

Figure 4 (a) shows that with an increment in the value of cutting speed, kerf taper increases due to the wall sides of the cutting width and obstruction of gas flow occurs due to the difficulties of blow out metal removal through the top and bottom kerf widths. Figure 4 (b) shows the increment in the value of kerf taper with the increase in the value of focus position from -1 mm to -4.2 mm. The nature of kerf taper variation is observed higher (significant) at low values of gas pressure while it is found smaller for high values of gas pressure with low cutting speeds as depicted in Figure 4(c). Therefore, in order to achieve a proper interface between the laser and workpiece material, to keep lower value of cutting speed is suggested. Furthermore, to proper regulate blow out the molten material from kerf, moderate value of gas pressure is suggested.

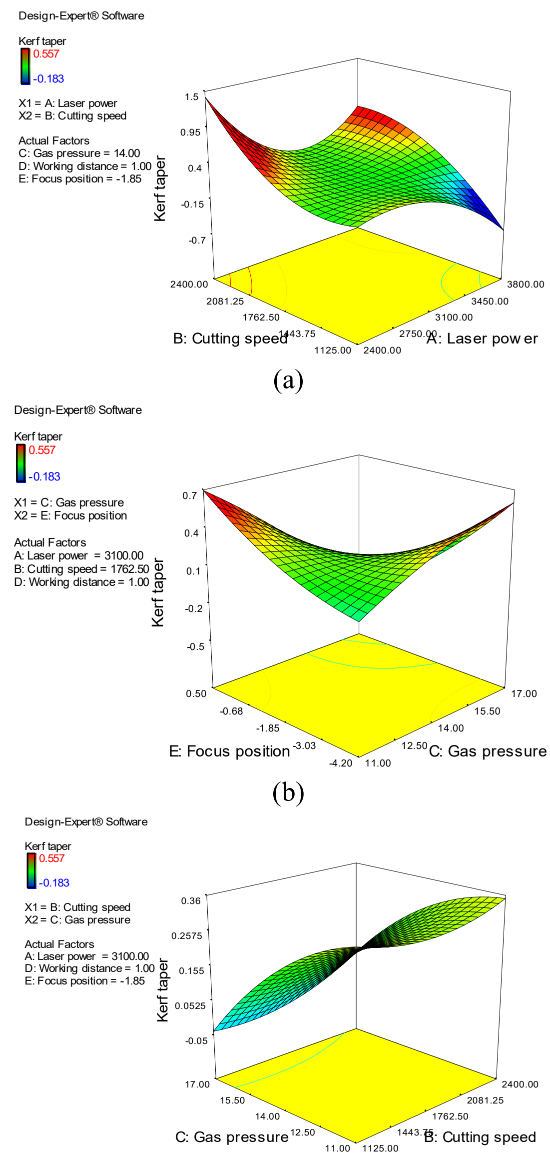


Fig. 4. Response surface plots of kerf taper for significant process parameters (a) laser power and cutting speed, (b) gas pressure and focus position, (c) cutting speed and gas pressure

It is observed from the Table 4 that the gas pressure, working distance and focus position with F-value as 1.1, 17.5 and 0.1 has least effect on kerf taper during the machining of material Hastelloy C-276 using laser machining process. Furthermore, the p – value as reported in Table 4 in the ANOVA analysis reveals their insignificance for the response kerf taper.

### 3.3 Desirability analysis and confirmation tests

In this section, desirability analysis using RSM is attempted for the experimental results of material Hastelloy C-276. In the desirability analysis, single response is considered at one time. A minimum level is set for performance characteristics kerf width and kerf taper which is required to be optimized. While the process parameters laser power, cutting speed, gas pressure, working distance and focus position are kept under range bounds. The obtained optimum process parameters are laser power as 2400 watts, cutting speed as 1762.5 mm/min, gas pressure as 14 bar, working distance as 1 mm and focus position as -1.85 mm for the response kerf width as 0.425 mm with the desirability value as 1. The obtained value of the desirability is 1 which signifies the improvement of the response kerf width. Similarly, using the desirability approach of RSM, the obtained optimum process parameters are laser power as 2805.69 watts, cutting speed as 1494.6 mm/min, gas pressure as 15.26 bar, working distance as 0.79 mm and focus position as -0.86 mm for the response kerf taper as 0.005 degree. The optimal conditions of laser machining process parameter are determined using RSM desirability analysis for the considered performance characteristics. However, the end step is to confirm the obtained results with the help of confirmatory tests. The obtained result of desirability analysis is validated by conducting the confirmation test experiments. The experimental confirmatory values obtained for the considered performance parameters kerf width and kerf taper as 0.443 and 0.0053 respectively. The corresponding value of error obtained as 0.042 and 0.06 respectively. This kind of effect study of process parameters were reported in literature for wire electric discharge and electric discharge machining process for Hastelloy and TiNiCu shape memory alloy respectively [31, 32].

## 4. OPTIMIZTION TECHNIQUES

In this section, the considered soft computing evolutionary optimization techniques are applied to the regression models that are obtain using the experimental results for the workpiece material Hastelloy C-276. It is observed from literature that the optimization techniques have found its applications in different domain like, path finding in sustainable design for energy supply systems [31] and network analysis [32]. On the basis of literature, the considered BH and KH algorithm are applied to laser machining process parameter optimization to see the effectiveness of the approach.

### 4.1 Blackhole algorithm

Black hole (BH) algorithm is based on the physics phenomenon of space “black hole”. It is developed and introduced by Hatamlou [33]. The algorithm is successfully implemented on six selected optimization problems to see the effectiveness of the BH algorithm. Black hole region is so much mass concentrated that has strong gravitational pull due to which even light cannot escape from it. This algorithm has less number of parameter to tune compared to other algorithms. It is a population-based algorithm in which star locations are generated randomly for evaluating the solution. The solution with highest fitness would be termed as “black hole” and other solutions will be considered as “normal stars”. The normal stars around the black hole are pulled at the end of initialization process. The black hole absorbs the star which comes very close to it and gets disappeared forever. After this, a new star (candidate solution) is randomly generated and placed in the search space to start a new search. The new population is evolved by moving all the candidates towards best candidate i.e., black hole based on their current location and replace those candidates within the range of the black hole.
The main steps of the BH algorithm steps are here in under [33]

***Step 1***: Initialize the population of stars randomly in search space.
***Step 2***: Evaluate the objective function for each star.
***Step 3***: Select the best star i.e. candidate solution as black hole and other as normal stars.
***Step 4***: Move each star towards black hole and change the location of stars.
***Step 5***: If a star reaches a position with the optimum value better than the value of black hole then exchange their positions.
***Step 6***: If a star crosses the limit of the black hole, replace it with a new star in a random position in the search space.
***Step 7***: If a termination criterion (a maximum number of iterations) is reached, exit the algorithm else go to step 3.

### 4.2 Krill herd algorithm

KH algorithm is a well-tested metaheuristic algorithms developed by Gandomi and Alavi [34]. KH is biologically inspired algorithm which mimics the behaviour of krill that are present in the deep sea. The algorithm is quite feasible to solve and obtain optimal solutions in complex optimization problems. It works on the basis of the density of krill and their individual distance from the food location. A Lagrangian model is given for KH algorithm as given in equation (4)

$$\frac{dX_i}{dx} = N_i + F_i + D_i \qquad (4)$$

Where Ni is the motion induced by each krill to other

individuals, Fi is krill's foraging motion for food and Di is the disturbance cause as physical diffusion.
The position of krill is updated using these three individual factors or motion. The final updated krill position dependent on time constant (*Δt*) is formulated as given in equation (5).

$$X_i(t + \Delta t) = X_i(t) + \Delta t \frac{dX_i}{dt} \qquad (5)$$

The main steps of the KH algorithm steps are here in under [34].

***Step 1***: Initialize the random population of the krill individuals. Set the control parameters such as foraging speed, maximum diffusion speed, and maximum induced speed.

***Step 2***: Evaluate the fitness value of each krill individual based on its position.

***Step 3***: Calculate the motion of each krill:

**i.** Motion induced by the existence of other krill individuals
**ii.** Foraging motion
**iii.** Physical diffusion

***Step 4***: Implement the genetic operators i.e. crossover and mutation.

***Step 5***: Update the krill individual position in the search space

***Step 6***: Evaluate the fitness value of each krill individual according to its new position.

***Step 7***: If termination criterion reached, stop the algorithm else go to step 3.

### 4.3 Optimization of Laser machining process

The effectiveness of the considered BH and KH algorithms are computed using equations (2) - (3). The performance parameters, i.e., kerf width and kerf taper are optimized separately. The objective to apply the evolutionary optimization algorithm is to achieve minimum value of the considered performance characteristics. The convergence graph for kerf width and kerf taper obtained are depicted in Figure 5 (a-b) respectively. The optimum values obtained using considered algorithms are shown in Table 5. The results of BH and KH algorithm for Laser cutting process when compared with RSM results (obtained in section 3), it is found that the results are quite aligned to each other for the performance parameters kerf width and kerf taper as shown in Table 5. The values of optimum process parameters for kerf width and kerf taper obtained using BH and KH algorithm are given in Table 5. As seen from the Figure 5, KH algorithm is converging faster compared to BH algorithm. Furthermore, the optimal solution obtained using KH algorithm is found better compared to BH algorithm with 200 iterations and number of trials as 10. The optimum solutions obtained for considered performance characteristics kerf width and kerf taper using KH has higher success rate compared to BH algorithm. The optimum results shown in Table 5 are rounded off as given Table 6, so that they can be easily tuned on the considered Laser machining process.

The mean, standard deviation and computational time obtained at the end trials (i.e., 10) for the convergence of kerf width and kerf taper using KH algorithm are {0.3496, 1.03 × $10^{-6}$}, {0.0061, 1.21 × $10^{-6}$} and {11.71, 10.64} respectively. Similarly, the mean, standard deviation and computational time obtained at the end trials (i.e., 10) for the convergence of kerf width and kerf taper using BH algorithm are {0.3827, 0.0063}, {0.0142, 0.0236} and {0.248, 0.268} respectively. While comparing the mean and standard deviation values of the KH and BH algorithms, the best values are obtained using KH algorithm.

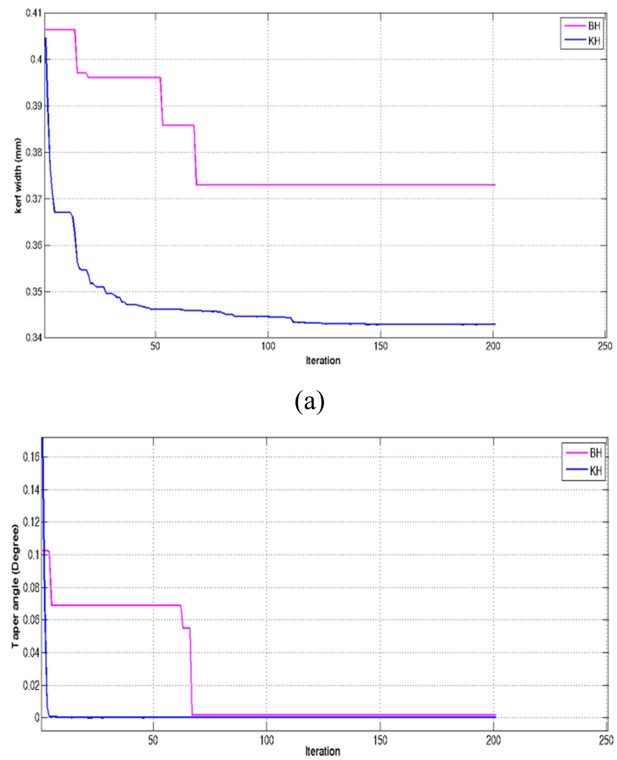


(a)

(b)

Fig. 5. Convergence of performance parameters using BH and KH algorithm (a) kerf width (b) kerf taper

The rounded off values of process parameters obtained using BH and KH algorithm are used to perform confirmatory test as shown in Table 7. The confirmatory test for the optimum results obtained using BH and KH algorithm shows that the percentage error for the considered performance characteristics is within 7 %. Furthermore, the results trend of BH and KH algorithm is found analogous with results obtained using RSM analysis. These values can be easily tuned on laser machining process to obtain desired output characteristics for the considered material Hastelloy C-276.

Table 5. Optimum results obtained using BH and KH algorithm

| Algorithm | Response | Response value | Laser power (watt) | | Cutting speed (mm/min) | | Gas pressure (bar) | | Working Distance (mm) | | Focus Position (mm) | |
|---|---|---|---|---|---|---|---|---|---|---|---|---|
| | | | *Coded* | *Actual* | *Coded* | *Actual* | *Coded* | *Actual* | *Coded* | *Actual* | *Coded* | *Actual* |
| **BHA** | kerf width (mm) | 0.3736 | -0.7935 | 2544.51 | 0.8196 | 2285.01 | -0.5043 | 12.4871 | -0.7391 | 0.6304 | -0.8697 | -3.8938 |
| | Kerf taper (degree) | 0.0005 | -0.9516 | 2433.89 | -0.7440 | 1288.39 | 0.5518 | 15.6556 | -0.2589 | 0.8705 | -0.6667 | -3.4167 |
| **KHA** | kerf width (mm) | 0.3428 | -1 | 2400 | 1 | 2400.00 | -0.4243 | 12.7271 | -1 | 0.5000 | -0.9988 | -4.1972 |
| | Kerf taper (degree) | $3.84 \times 10^{-6}$ | -0.9747 | 2417.69 | -0.8290 | 1234.14 | 0.4207 | 15.2622 | 0.3429 | 1.1714 | -0.1894 | -2.2952 |

Table 6. Feasible (Rounded-off) optimum results obtained using BH and KH algorithm

| Algorithm | Response | Response value | Laser power (watt) | | Cutting speed (mm/min) | | Gas pressure (bar) | | Working Distance (mm) | | Focus Position (mm) | |
|---|---|---|---|---|---|---|---|---|---|---|---|---|
| | | | *Coded* | *Actual* | *Coded* | *Actual* | *Coded* | *Actual* | *Coded* | *Actual* | *Coded* | *Actual* |
| **BHA** | kerf width (mm) | 0.3736 | -0.7929 | 2545 | 0.8196 | 2285 | -0.5000 | 12.5 | -0.7400 | 0.63 | -0.8681 | -3.89 |
| | Kerf taper (degree) | 0.0010 | -0.9514 | 2434 | -0.7440 | 1288 | 0.5666 | 15.7 | -0.2600 | 0.87 | -0.6681 | -3.42 |
| **KHA** | kerf width (mm) | 0.3428 | -1 | 2400 | 1 | 2400 | -0.4333 | 12.7 | -1 | 0.50 | -1 | -4.20 |
| | Kerf taper (degree) | 0.0005 | -0.9743 | 2418 | -0.8290 | 1234 | 0.4333 | 15.3 | 0.3400 | 1.17 | -0.1915 | -2.30 |

Table 7. Confirmatory test results for results obtained using BH and KH algorithm

| Algorithm | Response | Laser power (watt) | Cutting speed (mm/min) | Gas pressure (bar) | Working Distance (mm) | Focus Position (mm) | Response value | Confirmatory test result |
|---|---|---|---|---|---|---|---|---|
| **BH** | kerf width (mm) | 2545 | 2285 | 12.5 | 0.63 | -3.89 | 0.3736 | 0.3984 |
| | taper (degree) | 2434 | 1288 | 15.7 | 0.87 | -3.42 | 0.0010 | 0.0006 |
| **KH** | kerf width (mm) | 2400 | 2400 | 12.7 | 0.50 | -4.20 | 0.3428 | 0.3816 |
| | taper (degree) | 2418 | 1234 | 15.3 | 1.17 | -2.30 | 0.0005 | 0.0007 |

## 5. CONCLUSIONS

In this paper, the laser machining process parameters for material Hastelloy C-276 sheet are optimized using RSM and two selected optimization techniques, i.e., BH and KH algorithm. The main objective is to optimize output characteristics, i.e., kerf width and kerf taper for the selected range of process parameters laser power (watt), cutting speed (bar), gas pressure (bar), working distance (mm) and focus position (mm).

RSM is applied to obtain the optimum condition laser process parameters. The laser process parameters whose P-value is less than 0.05 have significant influence on considered kerf characteristics. The significance of laser process parameters is checked using ANOVA and it is observed that focus position and laser power has most influence on kerf width with percentage contribution 49.5 % and 13.9 % respectively. While the laser power has most influence on response kerf taper with percentage contribution 32.5 %. The optimum values obtained using RSM approach for kerf width and kerf taper are found as 0.425 mm and 0.005 degree. Regression models for kerf width and kerf taper are developed in terms of considered process parameters. These regression models are optimized using BH and KH algorithm to obtain the optimum value of considered process parameters for laser machining process. As these algorithms are well tested on the other problems of engineering, the use of these techniques is essential to obtain the approximate optimum solution for the considered process. Confirmatory test are performed to validate the experimental and optimization techniques results. The confirmatory test for the optimum results obtained using proposed methods shows that the percentage error for the considered performance characteristics is within 7 %.

## 6. REFERENCES

1. Guo, Y., Li, W. and Jawahir, I., (2009). *Surface integrity characterization and prediction in machining of hardened and difficult-to-machine alloys: a state-of-art research review and analysis*. Mach. Sci. Technol. **13**(4), 437-470.

2. M'Saoubi, R., Outeiro, J., Chandrasekaran, H. and Jawahir, I., (2008). *A review of surface integrity in machining and its impact on functional performance and life of machined products*. Int. J. Sus. Manuf. **1**(1/2) 203-209.

3. Ma, G., Wu, D., Niu, F. and Zou, H. (2015). *Microstructure evolution and mechanical property of pulsed laser welded Ni-based superalloy*. Opt. Lasers Engi. **72,** 39-46.

4. Manikandana, M., Arivazhagana, N., Rao, M.N. and Reddy, G.M. (2014). *Microstructure and mechanical properties of alloy C-276 weldments fabricated by continuous and pulsed current gas tungsten arc welding techniques*. J. Manuf. Process. **16**, 563–572.
5. Pusavec, F., Deshpande, A., Yang, S., M'Saoubi, R., Kopac, J., Dillon, O. and Jawahir, I. (2014). *Sustainable machining of high temperature Nickel alloy – Inconel 718: part 1 – predictive performance models*. J Cleaner Produc. **81**, 255-269.
6. Altin, A., Nalbant, M. and Taskesen, A. (2007). *The effects of cutting speed on tool wear and tool life when machining Inconel 718 with ceramic tools*. Mater. Des. **28**(9), 2518-2522.
7. Choudhury, I. A. and El-Baradie, M.A. (1998). *Machinability of nickel-base super alloys: a general review*. J Mater Process. Technol. **77**(1-3), 278-84.
8. Ezugwu, E., Wang, Z. and Machado, A. (1999). *The machinability of nickel-based alloys: a review*. J Mater. Process. Technol. **86**(1-3), 1-16.
9. Dudzinski, D., Devillez, A., Moufki, A., Larrouquère, D., Zerrouki, V. and Vigneau, J. (2004). *A review of developments towards dry and high speed machining of Inconel 718 alloy*. Int. J. Mach. Tools Manuf. **44**(4), 439-456.
10. Chryssolouris, G. (2010). *Laser machining: Theory and Practice*, (New York: Springer Science and Business Media).
11. Zheng, H., Han, Z., Chen, Z., Chen, W., Yeo, S. (1996). *Quality and cost comparisons between laser and waterjet cutting*. J Mater. Process. Technol. **62**(4), 294-298.
12. Ghany, K. and Newishy, M. (2005). *Cutting of 1.2mm thick austenitic stainless steel sheet using pulsed and CW Nd:YAG laser*. J. Mater. Process. Technol. **168**(3), 438-447.
13. Meijer, J. (2004). *Laser beam machining (LBM), state of the art and new opportunities*. J Mater. Process. Technol. **149**(1-3), 2-17.
14. Dubey, A.K., Yadava, V. (2008). *Laser beam machining—a review*. Int. J. Mach. Tools Manuf. **48**(6), 609-628.
15. Wang, Y., Yang, L. and Wang, N. (2002). *An investigation of laser-assisted machining of* $Al_2O_3$ *particle reinforced aluminum matrix composite*. J. Mater. Process. Technol. **129**(1-3), 268-272.
16. Hascalık, A. and Ay, M. (2013). $CO_2$ *laser cut quality of Inconel 718 nickel – based superalloy*. Opt. Laser Technol. **48**, 554-564.
17. Eltawahni, H. Olabi, A. and Benyounis, K. (2010). *Effect of process parameters and optimization of* $CO_2$ *laser cutting of ultra-high-performance polyethylene*. Mater. Des. **31**(8), 4029-4038.
18. Yilbas, B.S. (2001). *Effect of process parameters on the kerf width during the laser cutting process*. Proceedings of the Institution of Mech. Engi. Part B: J. Engi. Manuf. **215**(10), 1357- 1365.
19. Shrivastava, P.K. and Pandey, A. K. (2018). *Geometrical quality evaluation in laser cutting of inconel-718 sheet by using Taguchi based regression analysis and particle swarm optimization*. Infrared Phy. Technol. **89**, 369-380.
20. Shrivastava, P.K. and Pandey, A. K. (2018). *Parametric optimization of multiple quality characteristics in laser cutting of inconel-718 by using hybrid approach of multiple regression analysis and genetic algorithm*. Infrared Phy. Technol. **91**, 220- 232.
21. Stournaras, A., Stavropoulos, P., Salonitis, K. and Chryssolouris, G. (2009). *An investigation of quality in CO2 laser cutting of aluminum*. CIRP J. Manuf. Sci. Technol. **2** 61–69.
22. Kotadiya, D.J., Kapopara, J.M., Patel, A.R., Dalwadi, C.G. Pandya, D.H. (2018). *Parametric analysis of process parameter for Laser cutting process on SS-304*. Mater. Today: Proceed. **5**, 5384–5390.
23. Joshi, P. and Sharma, A. (2018). *Simultaneous optimization of kerf taper and heat affected zone in Nd-YAG laser cutting of Al 6061-T6 sheet using hybrid approach of grey relational analysis and fuzzy logic*. Prec. Engi. **54**, 302 – 313.
24. Boujelbene, M. (2018). *Influence of the* $CO_2$ *Laser cutting process parameters on the quadratic mean roughness Rq of the low carbon steel*. Proc. Manuf. **20**, 259–264.
25. Anghel, C., Gupta, K. and Jen, T.C. (2019). *Analysis and optimization of surface quality of stainless steel miniature gears manufactured by* $CO_2$ *Laser cutting*. Optik. **203**, 164049.
26. Rajesh, K.V., Raju, M. K., Rajesh, S. and Varma, N.S.K. (2019). *Effect of process parameters on machinability characteristics of* $CO_2$ *laser process used for cutting SS-304 Stainless steels*. Mater. Today: Proceed. **18**, 2065–2072.
27. Sharifi, M. and Akbari, M. (2019). *Experimental investigation of the effect of process parameters on cutting region temperature and cutting edge quality in laser cutting of AL6061T6 alloy*. Optik Int. J. Light Elec. **184**, 457–463.
28. Elsheikh, A.H., Deng, W. and Showaib, E.A. (2019). *Improving laser cutting quality of polymethyl methacrylate sheet: experimental investigation and optimization*. J. Mater. Res. Technol. (Article in press).
29. Montogomery, D.C. (2010) *Design and analysis of experiments*, (NJ, USA: John Wiley and Sons publisher).
30. Paneerselvam, R. (2012). *Design and analysis of experiment*, (India: PHI Learning Publisher).
31. Manoj I.V., Joy, R., Narendranath, S., Nedelcu, D. (2019). *Investigation of machining parameters on*

*corner accuracies for slant type taper triangle shaped profiles using WEDM on Hastelloy X*. IOP Conference Series: Mat. Sci. Engi. **591** (1), 012-022.
32. Abhinaba, R., Narendra, N.S., Dumitru, N. (2017). *Experimental investigation on variation of output responses of as cast TiNiCu shape memory alloys using EDM*. Int. J. Modern Manuf. Technol. **9** (1), 90-101
33. Majewski, D.E., Wirtz, M., Lampe, M. and Bardow, A. (2017). *Robust multi-objective optimization for sustainable design of distributed energy supply systems*. Comp. Chem. Engi. **102**, 26–39.
34. Rajabi-Bahaabadi, M., Shariat-Mohaymany, A., Babaei, M. and Ahn, C.W. (2015). *Multi-objective path finding in stochastic time-dependent road networks using non-dominated sorting genetic algorithm*. Exp. Sys. Appl. **42**(12), 5056–5064.
35. Hatamlou, A. (2013). Black hole: *A new heuristic optimization approach for data clustering*. Inf. Sci. **222**, 175–184.
36. Gandomi, A.H., Alavi, A. H. (2012). *Krill herd: A new bio-inspired optimization algorithm*. Comm. Nonlinear Sci. Numer. Simul. **17**(12), 4831–4845.

Received: February 23, 2020 / Accepted: June 15, 2020 / Paper available online: June 20, 2020 